Sensors & Actuators: B. Chemical 316 (2020) 128163

Contents lists available at ScienceDirect

Sensors and Actuators B: Chemical

journal homepage: www.elsevier.com/locate/snb

Enzyme-free colorimetric immunoassay for procalcitonin based on $MgFe_2O_4$ sacrificial probe with the Prussian blue production

Yueyuan Li[a], Lei Liu[a], Yaoguang Wang[b], Rong Ren[c], Dawei Fan[a], Dan Wu[a], Yu Du[a], Kun Xu[a,d,*], Xiang Ren[a,*], Qin Wei[a], Huangxian Ju[a]

[a] Collaborative Innovation Center for Green Chemical Manufacturing and Accurate Detection, Key Laboratory of Interfacial Reaction & Sensing Analysis in Universities of Shandong, School of Chemistry and Chemical Engineering, University of Jinan, Jinan 250022, PR China
[b] Shandong Provincial Key Laboratory of Molecular Engineering, School of Chemistry and Pharmaceutical Engineering, Qilu University of Technology (Shandong Academy of Sciences), Jinan 250353, PR China
[c] Department of Mathematical Sciences, Zibo Normal College, Zibo, Shandong 255130, PR China
[d] Anhui Dexinjia Biopharm Co., Ltd Mfg, No.9 Hexie Road, Biopark, Kaifaqu, Taihe, 236600 Anhui, PR China

ARTICLE INFO

Keywords:
Sacrificial
Prussian blue
Procalcitonin
$MgFe_2O_4$
Enzyme-free immunosorbent assay

ABSTRACT

An enzyme-free immunosorbent assay using $MgFe_2O_4$ modified with cysteine ($MgFe_2O_4$@Cys) as sacrificial probe for the detection of procalcitonin (PCT) was developed. $MgFe_2O_4$@Cys was linked with second antibody of PCT (Ab_2) by cysteine amino group and released Fe^{3+} under acidic conditions. Taking advantage of Fe^{3+} and $[Fe(CN)_6]^{4-}$ generating soluble Prussian blue (PB), a novel method of PCT determination was established by measuring the absorbance of the generated PB. Different from the traditional immunosensor detection mode, the enzyme-free colorimetric immunosensor in this work can not only avoid the interference of nano-enzymes or enzymes, but also has the advantages of rapid detection, low cost, high selectivity and sensitivity. Therefore, the developed immunosensor for PCT detection exhibited a wide linear response (0.0001–50 ng/mL) and a low detection limit (44.9 fg/mL). Additionally, the immunosensor exhibits satisfactory performance in human serum testing, which indicated its good application value in clinical diagnoses.

1. Introduction

In recent decades, the accurate identification and determination of disease biomarkers have become a research topic of interest in medical testing and diagnosis. Many studies have committed to developing more sensitive, portable, low cost, accurate and reliable strategies for biomarker detection [1–3]. Immunosensors have received significant investigative attention due to their advantages of rapid detection, low cost, high selectivity and sensitivity [4–6]. Therefore, immunosensors have been widely applied in pharmaceutical analysis, food monitoring, environmental protection and disease detection [7–10]. Enzyme-linked immunosorbent assay (ELISA) is one of the most popular bioassay methods [11,12], which has the properties of acceptable reactivity, selectivity, and specificity [13]. Nevertheless, the bioactivity of enzymes in ELISA systems is vulnerable and can be impacted by environmental factors, such as pH changes or temperature fluctuations of the surroundings [14,15]. To overcome the obstacles and achieve optimal enzymatic reactions for signal amplification, many efforts have been devoted to finding substituted enzymes for constructing conventional ELISA systems. For instance, Todoroki et al. employed a chemically stable DNA aptamer and an HRP − protein A conjugate analysis of a therapeutic human monoclonal antibody; in this work, the colorimetric result was detected through HRP activity [16]. Based on the Pt staining to stain Au nanoparticles (NPs) with Ag and Pt bimetallic shells, Yang's group designed a pressure-based bioassay that significantly improved the sensitivity compared with that of protein enzyme-based detection [17]. Modified ELISA has become one of the most prospective methods due to its easy operation, direct readout by the naked eye, and high sensitivity. To date, nano-enzymes, such as Pd, Pt or Au NPs and enzyme-based nanocarriers, have been extensively applied and demonstrated as signal markers in bioassays [18–20]. However, the signal output still depends on the bioactivity of the nano-enzymes and enzymes. Therefore, avoiding the defects of nano-enzymes or enzymes is an important issue for improving the sensitivity of immunosensors.

Magnesium ferrite ($MgFe_2O_4$) is one of the most attractive magnetic

* Corresponding authors at: Collaborative Innovation Center for Green Chemical Manufacturing and Accurate Detection, Key Laboratory of Interfacial Reaction & Sensing Analysis in Universities of Shandong, School of Chemistry and Chemical Engineering, University of Jinan, Jinan 250022, PR China.
E-mail addresses: ahxukun@163.com (K. Xu), chem_renx@163.com (X. Ren).

https://doi.org/10.1016/j.snb.2020.128163
Received 13 November 2019; Received in revised form 20 April 2020; Accepted 20 April 2020
Available online 26 April 2020
0925-4005/

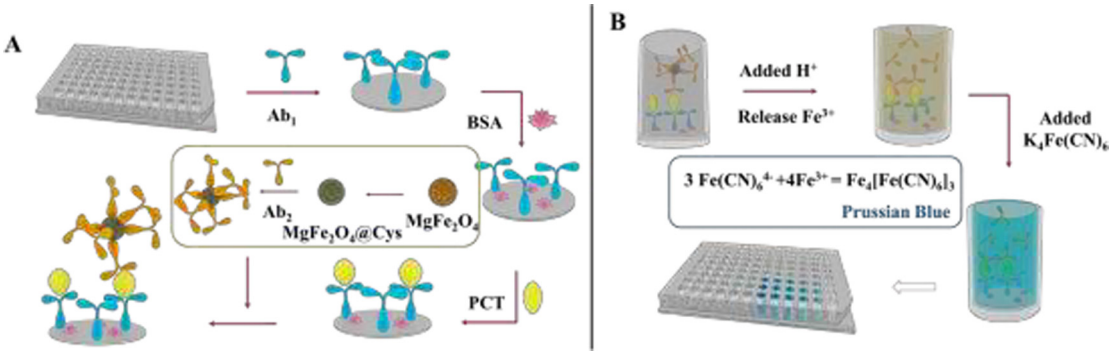

Scheme 1. (A) Illustration of the fabrication process of the sacrificial immunosensor for the detection of PCT. (B) The reaction involved releasing Fe^{3+} by H^+ and visual detection in a 96-microwell plate.

oxides with spinel structures [21]. The compound exhibited high stability, a developed surface, a small particle size, and excellent magnetic characteristics [22], and its broad applications have been achieved in the areas of fuel, environmental conservation, gas sensors, and photocatalysis [23–26]. We first introduce $MgFe_2O_4$ as a sacrificial probe of an immunosensor, which is expected to be an excellent strategy for biomarker detection. The sacrificial probe strategy consists of the following considerations: first, magnetic $MgFe_2O_4$ nanoparticles were easily coated with cysteine (Cys) to form $MgFe_2O_4$@Cys that can link with secondary antibodies (Ab_2) with the assistance of 1-ethyl-3-(3-dimethylaminopropyl)carbodiimide/N-hydroxysuccinimide (EDC/NHS) as crosslinkers. Second, $MgFe_2O_4$ as a magnetic oxide, can be dissolved under acidic condition through sacrificing themselves and released Fe^{3+}. Third, Fe^{3+} can easily react with $[Fe(CN)_6]^{4-}$ to generate soluble Prussian blue (PB, $K_{sp} = 10^{-40}$) [27]. Finally, the obviation of enzyme in our assay cuts down the cost of the assay and avoids the issues in conventional ELISA, such as enzyme denaturation and variation of enzymatic activities with temperature. Based on the above considerations, a new method for procalcitonin (PCT) determination in human serum was established by measuring the generated PB absorbance [28]. As a typical biomarker of sepsis in human serum, PCT plays a vital role in assessing the severity and progression of sepsis [29]. $MgFe_2O_4$ was explored as an efficient, sacrificial and reliable probe to fabricate a visible immunosensor for PCT detection. The fabricated immunosensor provided a new direction for biomarker detection research.

2. Material and methods

2.1. Preparation of $MgFe_2O_4$ nanomaterials

$MgFe_2O_4$ was prepared according to the report of Kang et al. [30]. First, solutions A and B were prepared. 0.1 g of PVP (polyvinylpyrrolidone, $K = 30$) was added to 60 mL of ethylene glycol and ultrasonication for 30 min to form a uniform solution denoted as A. Solution B was prepared by adding 0.64 g of $Mg(NO_3)_2{\cdot}6H_2O$ and 0.808 g of $Fe(NO_3)_3{\cdot}10H_2O$ into 10 mL of ethylene glycol. Subsequently, solution B was added into solution A under stirring to form a homogenous solution. Afterwards, 3.6 g of CH_3COONa and 1.0 g polyethylene glycol ($M_w = 2000$) were added to the mixture. The mixture was dissolved by ultrasonication and stirring to form a homogeneous solution. Then, the mixture was transferred to an autoclave and maintained at 200 °C for 24 h. After cool to room temperature, the solid was washed with ethyl alcohol and water by magnetic separation. Finally, the $MgFe_2O_4$ was obtained after drying under vacuum.

2.2. Preparation of $MgFe_2O_4$@Cys

$MgFe_2O_4$@Cys was prepared as follows: At first, 0.05 g of $MgFe_2O_4$ was dispersed in 25 mL of water under ultrasonication. The pH was adjusted to 4–5 with a 2 mol/L hydrochloric acid solution. Subsequently, 12.5 mL of L-cysteine (1 mg/mL) was added dropwise to the mixture under ultrasonication for 30 min. The product was washed by ethyl alcohol and water with magnetic separation. Finally, the $MgFe_2O_4$@Cys was obtained after drying under vacuum.

2.3. Preparation of $MgFe_2O_4$@Cys-Ab_2

The preparation procedure of $MgFe_2O_4$@Cys-Ab_2 was as follows: first, 1 mL of $MgFe_2O_4$@Cys (3.5 mg/mL) solution was prepared. Next, 1 mL of Ab_2 (10 μg/mL) and 2 mL of EDC (75 mmol/L)/NHS (15 mmol/L) were added to the solution and incubated at 4 °C overnight. $MgFe_2O_4$@Cys-Ab_2 was obtained after magnetic separation and dispersed in 1 mL of PBS (pH = 7.4).

2.4. Procedure of colorimetric immunoassay and measurements

First, 100 μL of PCT primary antibody (Ab_1, 1 μg/mL) was dropped onto a 96-microwell plate and incubated overnight at 4 °C. After each well was washed with PBS (pH = 7.4) for three times, the wells were treated with 1% BSA (100 μL, 1 h) to block the nonspecific active sites. Then, the free BSA was removed with PBS. Subsequently, 100 μL of PCT at different concentrations was added and incubated at 37 °C for 1 h. Subsequently, $MgFe_2O_4$@Cys-Ab_2 (100 μL, 3.5 mg/mL) was added and incubated at 37 °C for 1 h. Similarly, the wells were washed three times with PBS. Next, 100 μL of HCl solution (1.2 mol/L) was put into each well for 10 min to cause Fe^{3+} release from $MgFe_2O_4$ under shaking. Finally, 100 μL of $K_4Fe(CN)_6$ (0.5 mol/L) solution was added to the wells and reacted for 10 min under gentle shaking. Then, the absorbance values were recorded.

3. Results and discussion

The fabrication and visualization processes of the visible immunosensor are demonstrated in Scheme 1. As illustrated in Scheme 1A, the sacrificial probe ($MgFe_2O_4$) was modified with Cys. Therefore, the secondary antibody (Ab_2) of PCT can be easily captured on the probe surface by the activation of EDC/NHS. The resultant $MgFe_2O_4$@Cys-Ab_2 bioconjugate was used as a sacrificial probe for PCT detection. As briefly shown in Scheme 1B, after adding a strong acidic solution into the well, Fe^{3+} was released from $MgFe_2O_4$. Upon the addition of $K_4[Fe(CN)_6]$, the chemical reaction of Fe^{3+} and $[Fe(CN)_6]^{4-}$ resulted in a distinct color change. With increasing of PCT concentration, the amount of immobilized $MgFe_2O_4$@Cys-Ab_2 on the 96-microwell plate increased. The color variations of the solution reflect the PCT concentration during detection.

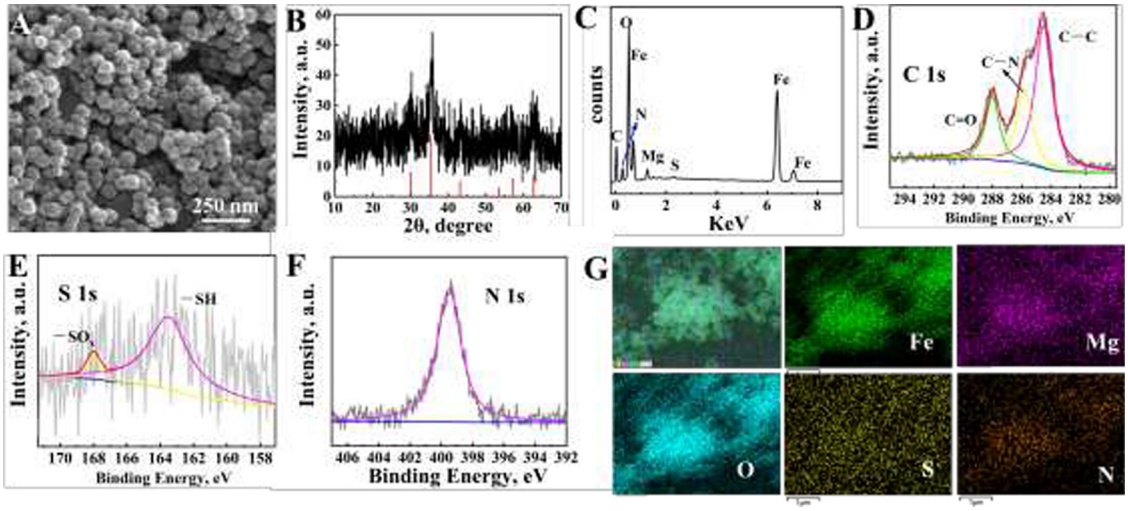

Fig. 1. SEM (A) and XRD (B) images of $MgFe_2O_4$. EDS (C) spectrum of $MgFe_2O_4$@Cys. The XPS spectra of C 1s (D), S 1s (E) and N 1s (F) in $MgFe_2O_4$@Cys. SEM elemental mapping of $MgFe_2O_4$@Cys (G).

3.1. Characterization of $MgFe_2O_4$ and $MgFe_2O_4$@Cys

The morphology of $MgFe_2O_4$ was characterized by scanning electron microscopy (SEM). As shown in Fig. 1A, the $MgFe_2O_4$ particles with rough surfaces have average diameters of approximately 70 nm. Then, the XRD pattern was utilized to characterize the crystallinity of $MgFe_2O_4$. As displayed in Fig. 1B, several peaks at 2θ = 30.3°, 35.7°, 43.3°, 57.2° and 62.9° were found to correspond to the (200), (311), (400), (511) and (440) planes of $MgFe_2O_4$ (JCPDS No: 73-1720), confirming the successful preparation of $MgFe_2O_4$ [21]. Since Cys played an important role in connecting Ab_2 during the fabrication of the immunosensor, EDS spectra (Fig. 1C) was employed to prove the successful preparation of $MgFe_2O_4$@Cys, in which the three elements of C, N and S were observed, confirming that Cys was successfully linked to the particle surface. Moreover, X–ray photoelectron spectroscopy (XPS) of $MgFe_2O_4$ (Fig. S1) and $MgFe_2O_4$@Cys (Fig. S2) was performed. The XPS spectra of Fe 2p are shown in Fig. S3 and display six peaks, which represent $2p_{3/2}$ of Fe^{2+} (710.3 eV) and Fe^{3+} (712.3 eV), 2p1/2 of Fe^{2+} (724 eV) and Fe^{3+} (727 eV), and the accompanying satellite peaks (denoted as "Sat.") at 718.7 and 732.5 eV [31]. The Mg 1 s signal is shown in Fig. S4 which was observed at 1304 eV [32]. The O 1s spectrum was assigned to 529.7 and 531.1 eV and is shown in Fig. S5. The former refers to oxygen in the lattice (M-O), such as in the bonds of oxygen atoms with magnesium and iron atoms (Mg–O, Fe–O). The latter was attributed to metal hydroxides or hydroxyl groups (OH–) [30]. The spectrum of C 1s (Fig. 1D) was assigned to three peaks, which were attributed to C-C (sp^2, 284.5 eV), C–N (285.8 eV) and C = O bonds (288 eV) [33]. The spectrum of S (Fig. 1E) was divided into two different peaks, which were 163.5 and 168 eV for -SH and the residual $-SO_x$ species [34]. As expected, there was a significant, new peak at 399.4 eV, which was assigned to N 1s (Fig. 1F) [35]. No obvious difference was observed in the SEM image of $MgFe_2O_4$@Cys (Fig. S6) and $MgFe_2O_4$ (Fig. 1A). The SEM elemental mapping of $MgFe_2O_4$@Cys is shown in Fig. 1G, which can further verify the presence of N and S and the uniform distribution of Fe, Mg and O. The detection methods proved Cys was successfully linked to $MgFe_2O_4$ and that the sacrificial visible probe of $MgFe_2O_4$@Cys can link with Ab_2 by Cys.

3.2. Characterization of the immunosensor

The mechanism of the sacrificial probe can be observed in the UV-vis spectra in Fig. 2A. The absorbance of $MgFe_2O_4$ was approximately observed in the 400 nm range (curve a) [36]. For the $MgFe_2O_4$@Cys nanocomposite (curve b), its absorption moved in the visible region due to the presence of Cys [36]. After adding H^+ into the well to dissolve $MgFe_2O_4$ with the release of Fe^{3+}, the absorption of $MgFe_2O_4$ in curve c disappeared, and a new peak appeared at approximately 350 nm [37]. Finally, a new peak (curve d) appeared at approximately 720 nm after adding a $K_4[Fe(CN)_6]$ solution to the well [38]. The same conditions were used for the fabrication of the immunosensor, but not for Ab_1 or PCT. The detection results are showed in Fig. 2B and C, which confirmed that if there was no Ab_1 or antigen, the immunosensor can be not successfully fabricated.

3.3. Detection conditions

Considering that Fe^{3+} was released from $MgFe_2O_4$ by the addition of HCl, the concentration of HCl and the reaction time play a key role in colorimetric detection. To conduct the optimization experiment, the same condition of PCT (0.1 ng/mL) was used for PCT detection. As the probe of the immunosensor, the concentration of $MgFe_2O_4$@Cys-Ab_2 is a crucial factor. As shown in Fig. 2D, as the concentration of $MgFe_2O_4$@Cys-Ab_2 increased, the absorbance value plateaued at 2.5 mg/mL. The concentration of $MgFe_2O_4$@Cys-Ab_2 was optimal at 2.5 mg/mL. As shown in Fig. 2E, the optimum concentration and reaction time of HCl are 1.2 mol/L and 10 min, respectively. In addition, the impact of the concentration of $K_4Fe(CN)_6$ and reaction time (Fig. 2F) is also important. To ensure complete reaction, the optimal concentration and reaction time of $K_4Fe(CN)_6$ were determined to be 50 mmol/L and 10 min, respectively.

3.4. Immunoassay performance

Under the optimized conditions, the developed immunosensor was used to detect PCT at different concentrations, which presented a wide linear chromogenic response range from 0.0001 to 50 ng/mL. As illustrated in Fig. 3A and B, the obtained linear relationship equation between the concentration and absorbance was A = 2.28 + 0.486lgc (ng/mL, r = 0.994), and the detection limit was 44.9 fg/mL (Supporting information S-5) [39]. Compared to the reported work (Table S1), the proposed immunosensor exhibited a low limit of detection and wide linear range for PCT detection.

3.5. Specificity, reproducibility and stability

To characterize the specificity, carcino-embryonic antigen (CEA), alpha fetoprotein (AFP), insulin and glucose were used as four common interferences for the specificity examination. As shown in Fig. 3C, the

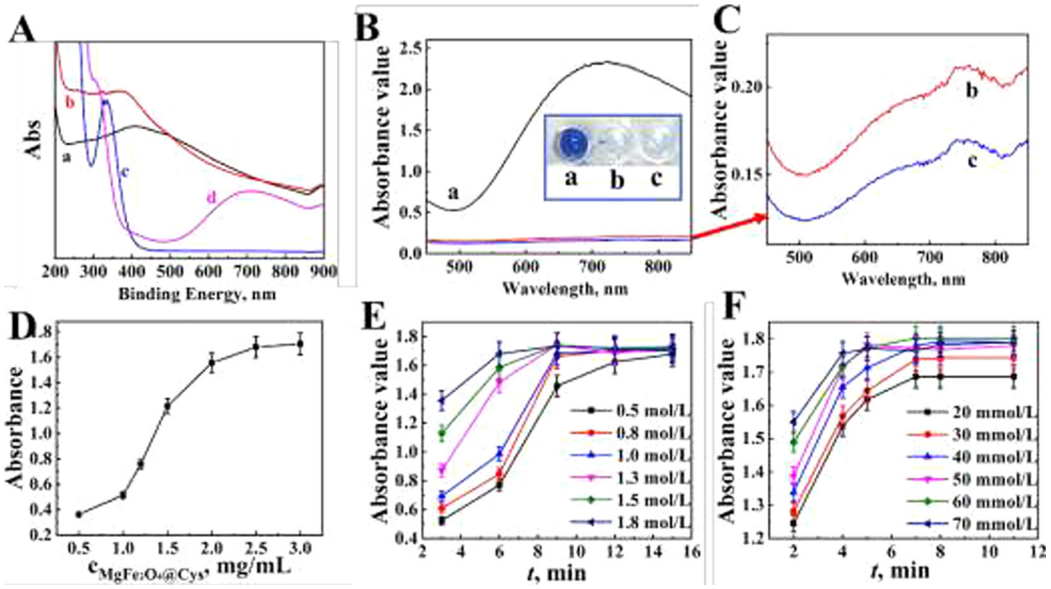

Fig. 2. (A) UV–vis spectra of aqueous solutions including $MgFe_2O_4$ (a), $MgFe_2O_4$@Cys (b), $MgFe_2O_4$@Cys + H^+ (c) and $MgFe_2O_4$@Cys + H^+ + $[Fe(CN)_6]^{4-}$ (d). (B) The absorbance value of the immunosensor fabricated with PCT (1.0 ng/mL, curve a). Insert: photos of the immunosensors. (C) The absorbance values of the immunosensor fabricated without PCT (b) and without Ab_1 (c). The optimal experiment of the concentration of $MgFe_2O_4$@Cys (D), the concentration and reaction time of HCl (E), and the concentration and reaction time of $K_4Fe(CN)_6$ (F).

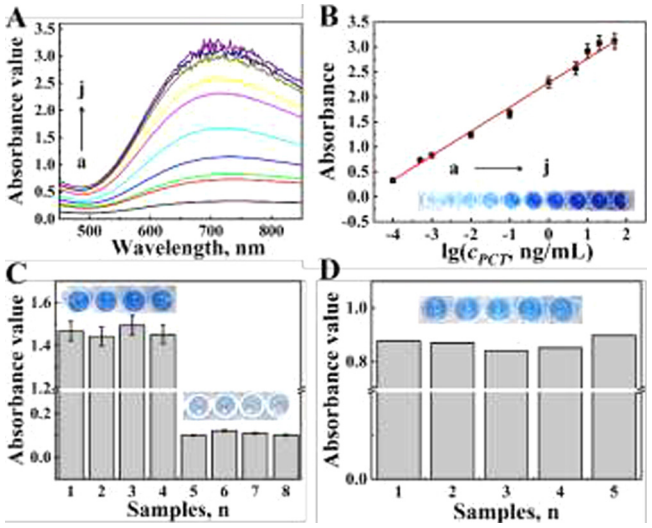

Fig. 3. (A) Absorbance values of the immunosensor subjected to different concentrations of PCT. (B) The linear relationship equation between absorbance and the different concentrations of PCT (a–j: 0.0001, 0.0005, 0.001, 0.01, 0.1, 1, 5, 10, 20 and 50 ng/mL). (C) Absorbance values of the immunosensor with (1) 20 pg/mL PCT + 0.2 ng/mL CEA, (2) 20 pg/mL PCT + 0.2 ng/mL AFP, (3) 20 pg/mL PCT + 0.2 ng/mL insulin, (4) 20 pg/mL PCT + 0.2 ng/mL glucose, (5) 0.2 ng/mL CEA, (6) 0.2 ng/mL AFP, (7) 0.2 ng/mL insulin and (8) 0.2 ng/mL glucose. (D) The reproducibility of the proposed immunosensor incubated with 1 pg/mL PCT. (Error bar = SD, n = 5.)

absorbance values of the samples containing PCT (samples 1–4) were much higher than those of the samples containing interferences (samples 5–8). The results indicated that the immunosensor had favorable specificity for PCT detection. The reproducibility of the fabricated immunosensor was tested with 1 pg/mL PCT by five independent experiments, and the results are shown in Fig. 3D, revealing that the reproducibility of the proposed immunosensor was acceptable. Moreover, the stability of the immunosensor was analyzed by storage at 4 °C. The absorbance value of the immunosensor decreased by approximately 3.6% and 7.9% of the original value after storage for 7 and 15 days, respectively. The results suggested that the immunosensor had satisfactory stability.

3.6. Real sample analysis

To validate the feasibility of the immunosensor, healthy human serum was analyzed using the proposed immunosensor in a spike recovery test. As shown in Table 1, different concentrations of PCT (0.02, 0.1, 0.5 and 20 ng/mL) were added to the sample and the healthy human serum was diluted two times. The recoveries of the results were in the range of 96.6%–106.4%, and the RSD was 4.3%~4.9%. In addition, healthy human serum was detected by ELISA and evaluated by *F-test* and *t-test* (Table S2). The calculated values were F = 2.05 and t = 0.167 (df ≈ 9), which implied that the two detection methods did not have any significant difference and that the system error can be ignored. Through real sample analysis, the proposed immunosensor was validated to be applicable for the detection of PCT in serum samples and has application value in clinical settings.

Table 1
The spike recovery test of the immunosensor in human serum sample.

Added, ng/mL	Found, ng/mL	Average, ng/mL	RSD, %	Recovery, %
0.02	0.039, 0.042, 0.044, 0.041, 0.044	0.04	4.9	106.4
0.10	0.114, 0.122, 0.117, 0.111, 0.122	0.12	4.3	96.6
0.50	0.583, 0.514, 0.534, 0.562, 0.538	0.55	4.9	105.1
20.0	20.70, 19.58, 20.29, 21.60, 19.10	20.25	4.8	101.1

4. Conclusion

In summary, a new colorimetric immunosensor method was used for the detection of PCT based on the sacrificial probe $MgFe_2O_4$@Cys. The magnetic material of $MgFe_2O_4$ releases Fe^{3+} under acidic conditions, and its reaction with $[Fe(CN)_6]^{4-}$ generates PB. This new mode of immunosensing can effectively avoid the interference of nano-enzymes or enzymes and achieve sensitivity detection of PCT. Simultaneously, this immunosensor is a promising technique for use in clinical diagnosis.

Author contributions

Y.Y. L., L. L., Y.G. W conceived and designed the experiments., Y.Y. L., D.W. F., D. W., Y. D. performed the experiments, analyzed the data and wrote the first draft of the manuscript. K. X., X. R., Q. W. and H.X. J. contributed substantially to revisions. All the authors discussed the results and commented on the manuscript.

Declaration of Competing Interest

The authors declare that they have no known competing financial interests or personal relationships that could have appeared to influence the work reported in this paper.

Acknowledgments

This work was supported by the National Key Scientific Instrument and Equipment Development Project of China (No.21627809), theNational Natural Science Foundation of China (Nos.21575050,21775054,21505051), theNatural Science Foundation of Shandong Province(No. ZR2016JL013), the Special Foundation for Taishan Scholar Professorship of Shandong Province (No.ts201712052), theJinan Scientific Research Leader Workshop Project(2018GXRC024) and the Program for Scientific Research Innovation Team in Colleges and Universities of Shandong Province.

Appendix A. Supplementary data

Supplementary material related to this article can be found, in the online version, at doi:https://doi.org/10.1016/j.snb.2020.128163.

References

[1] L. Jiao, W. Xu, H. Yan, Y. Wu, W. Gu, H. Li, et al., A dopamine-induced Au hydrogel nanozyme for enhanced biomimetic catalysis, Chem. Commun. 55 (2019) 9865–9868.
[2] F.-R. Liu, J.-T. Cao, Y.-L. Wang, X.-L. Fu, S.-W. Ren, Y.-M. Liu, A spatial-resolved electrochemiluminescence aptasensor for carcinoembryonic antigen detection in a double-check mode, Sens. Actuators B Chem. 276 (2018) 173–179.
[3] J. Xue, L. Yang, Y. Jia, H. Wang, N. Zhang, X. Ren, et al., Electrochemiluminescence double quenching system based on novel emitter $GdPO_4$: Eu with Low-excited positive potential for ultrasensitive procalcitonin detection, ACS Sens. 4 (2019) 2825–2831.
[4] S. Park, J. Kim, S. Kim, G. Kim, N.-S. Lee, Y.H. Yoon, et al., Combined signal amplification using a propagating cascade reaction and a redox cycling reaction for sensitive thyroid-stimulating hormone detection, Anal. Chem. 91 (2019) 7894–7901.
[5] G. Zhao, Y. Wang, X. Li, Q. Yue, X. Dong, B. Du, et al., Dual-quenching electrochemiluminescence strategy based on three-dimensional metal–organic frameworks for ultrasensitive detection of amyloid-β, Anal. Chem. 91 (2019) 1989–1996.
[6] D. Qin, X. Jiang, G. Mo, J. Feng, C. Yu, B. Deng, A novel carbon quantum dots signal amplification strategy coupled with sandwich electrochemiluminescence immunosensor for the detection of CA15-3 in human serum, ACS Sens. 4 (2019) 504–512.
[7] D. Yu, B. Blankert, J.C. Viré, J.M. Kauffmann, Biosensors in drug discovery and drug analysis, Anal. Lett. 38 (2005) 1687–1701.
[8] M. Lv, Y. Liu, J. Geng, X. Kou, Z. Xin, D. Yang, Engineering nanomaterials-based biosensors for food safety detection, Biosens. Bioelectron. 106 (2018) 122–128.
[9] S. Dong, S. Wang, E. Gyimah, N. Zhu, K. Wang, X. Wu, et al., A novel electrochemical immunosensor based on catalase functionalized AuNPs-loaded self-assembled polymer nanospheres for ultrasensitive detection of tetrabromobisphenol A bis(2-hydroxyethyl)ether, Anal. Chim. Acta 1048 (2019) 50–57.
[10] L. Tang, S. Li, L. Xu, W. Ma, H. Kuang, L. Wang, et al., Chirality-based Au@Ag nanorod dimers sensor for ultrasensitive PSA detection, ACS Appl. Mater. Interfaces 7 (2015) 12708–12712.
[11] B.K. Van Weemen, A.H. Schuurs, Immunoassay using antigen-enzyme conjugates, FEBS Lett. 15 (1971) 232–236.
[12] T. Wei, D. Du, M.-J. Zhu, Y. Lin, Z. Dai, An improved ultrasensitive enzyme-linked immunosorbent assay using hydrangea-like antibody–enzyme–inorganic three-in-one nanocomposites, ACS Appl. Mater. Interfaces 8 (2016) 6329–6335.
[13] S. Tong, B. Ren, Z. Zheng, H. Shen, G. Bao, Tiny grains give huge gains: nanocrystal-based signal amplification for biomolecule detection, ACS Nano 7 (2013) 5142–5150.
[14] M. Pita, V. Privman, M.A. Arugula, D. Melnikov, V. Bocharova, E. Katz, Towards biochemical filters with a sigmoidal response to pH changes: buffered biocatalytic signal transduction, Phys. Chem. Chem. Phys. 13 (2011) 4507–4513.
[15] R.-J. Yu, W. Ma, X.-Y. Liu, H.-Y. Jin, H.-X. Han, H.-Y. Wang, et al., Metal-linked immunosorbent assay (MeLISA): the enzyme-free alternative to ELISA for biomarker detection in serum, Theranostics 6 (2016) 1732–1739.
[16] T. Yamada, T. Saito, Y. Hill, Y. Shimizu, K. Tsukakoshi, H. Mizuno, et al., High-throughput bioanalysis of bevacizumab in human plasma based on enzyme-linked aptamer assay using anti-idiotype DNA aptamer, Anal. Chem. 91 (2019) 3125–3130.
[17] J. Li, F. Liu, Z. Zhu, D. Liu, X. Chen, Y. Song, et al., In situ Pt staining method for simple, stable, and sensitive pressure-based bioassays, ACS Appl. Mater. Interfaces 10 (2018) 13390–13396.
[18] W.J. Zhou, W.B. Liang, X. Li, Y.Q. Chai, R. Yuan, Y. Xiang, MicroRNA-triggered, cascaded and catalytic self-assembly of functional "DNAzyme ferris wheel" nanostructures for highly sensitive colorimetric detection of cancer cells, Nanoscale 7 (2015) 9055–9061.
[19] W. Zhou, J. Su, Y. Chai, R. Yuan, Y. Xiang, Naked eye detection of trace cancer biomarkers based on biobarcode and enzyme-assisted DNA recycling hybrid amplifications, Biosens. Bioelectron. 53 (2014) 494–498.
[20] L. Jiao, H. Yan, W. Xu, Y. Wu, W. Gu, H. Li, et al., Self-assembly of all-inclusive allochroic nanoparticles for the improved ELISA, Anal. Chem. 91 (2019) 8461–8465.
[21] N.R. Su, P. Lv, M. Li, X. Zhang, M. Li, J. Niu, Fabrication of $MgFe_2O_4$–ZnO heterojunction photocatalysts for application of organic pollutants, Mater. Lett. 122 (2014) 201–204.
[22] S. Verma, P.A. Joy, Y.B. Khollam, H.S. Potdar, S.B. Deshpande, Synthesis of nanosized $MgFe_2O_4$ powders by microwave hydrothermal method, Mater. Lett. 58 (2004) 1092–1095.
[23] Y. Liu, P. Zhang, M. Fan, P. Jiang, Biodiesel production from soybean oil catalyzed by magnetic nanoparticle $MgFe_2O_4$@CaO, Fuel 164 (2016) 314–321.
[24] L. Lu, J. Li, J. Yu, P. Song, D.H.L. Ng, A hierarchically porous $MgFe_2O_4$/γ-Fe_2O_3 magnetic microspheres for efficient removals of dye and pharmaceutical from water, Chem. Eng. J. 283 (2016) 524–534.
[25] Y.-L. Liu, Z.-M. Liu, Y. Yang, H.-F. Yang, G.-L. Shen, R.-Q. Yu, Simple synthesis of $MgFe_2O_4$ nanoparticles as gas sensing materials, Sens. Actuators B Chem. 107 (2005) 600–604.
[26] J. Luo, X. Zhou, L. Ma, X. Xu, J. Wu, H. Liang, Enhanced photodegradation activity of methyl orange over Ag_2CrO_4/SnS_2 composites under visible light irradiation, Mater. Res. Bull. 77 (2016) 291–299.
[27] D.E. Stilwell, K.H. Park, M.H. Miles, Electrochemical studies of the factors influencing the cycle stability of Prussian blue films, J. Appl. Electrochem. 22 (1992) 325–331.
[28] L. Shi, H. Huang, L. Sun, Y. Lu, B. Du, Y. Mao, et al., $[Fe(CN)_6]^{4-}$ decorated mesoporous gelatin thin films for colorimetric detection and as sorbents of heavy metal ions, Dalton Trans. 42 (2013) 13265–13272.
[29] F. Liu, G. Xiang, R. Yuan, X. Chen, F. Luo, D. Jiang, et al., Procalcitonin sensitive detection based on graphene–gold nanocomposite film sensor platform and single-walled carbon nanohorns/hollow Pt chains complex as signal tags, Biosens. Bioelectron. 60 (2014) 210–217.
[30] D. Kang, X. Yu, M. Ge, W. Song, One-step fabrication and characterization of hierarchical $MgFe_2O_4$ microspheres and their application for lead removal, Micropor. Mesopor. Mater. 207 (2015) 170–178.
[31] Y. Diao, Z. Yan, M. Guo, X. Wang, Magnetic multi-metal Co-doped magnesium ferrite nanoparticles: an efficient visible light-assisted heterogeneous fenton-like catalyst synthesized from saprolite laterite ore, J. Hazard. Mater. 344 (2018) 829–838.
[32] Y. Shen, Y. Wu, X. Li, Q. Zhao, Y. Hou, One-pot synthesis of $MgFe_2O_4$ nanospheres by solvothermal method, Mater. Lett. 96 (2013) 85–88.
[33] J.-H. Yang, V. Penmatsa, S. Tajima, H. Kawarada, C. Wang, Direct amination on 3-dimensional pyrolyzed carbon micropattern surface for DNA detection, Mater. Lett. 63 (2009) 2680–2683.
[34] K.T.V. Marcia, R.M. Chaves, Ronald D. DeLaune, Robert P. Gambrell, Pedro M. Buchler, Modification of Mackinawite with L-Cysteine: Synthesis, Characterization, and Implications to Mercury Immobilization in Sediment, in: S.S. Ginsberg (Ed.), Sediment Transport, InTech, Croatia, 2011, p. 313.
[35] M. Rodrigo Petoral, Kajsa Uvdal, Arg-Cys and Arg-cysteamine adsorbed on gold and the G-protein-adsorbate Interaction, Colloid Surf. B 25 (2002) 335–346.
[36] N.-U. Ain, W. Shaheen, B. Bashir, N.M. Abdelsalam, M.F. Warsi, M.A. Khan, et al., $_2$Electrical, magnetic and photoelectrochemical activity of rGO/$MgFeO_4$ nanocomposites under visible light irradiation, Ceram. Int. 42 (2016) 12401–12408.
[37] R.B. Hernández, A.P. Franco, O.R. Yola, A. López-Delgado, J. Felcman, M.A.L. Recio, et al., Coordination study of chitosan and Fe^{3+}, J. Mol. Struct. 877 (2008) 89–99.

[38] T. Koshiyama, M. Tanaka, M. Honjo, Y. Fukunaga, T. Okamura, M. Ohba, Direct synthesis of Prussian blue nanoparticles in liposomes incorporating natural Ion channels for Cs^+ adsorption and particle size control, Langmuir 34 (2018) 1666–1672.
[39] IUPAC, Nomenclature, symbols, units and their usage in spectrochemical analysis - II. Data interpretation, Pure Appl. Chem. 33 (2008) 241–245.

Yueyuan Li is a current PhD student, studies in School of Chemistry and Chemical Engineering, University of Jinan. She is working on constructing immunosensor.

Lei Liu received the PhD degree from China University of Geosciences (Beijing), Beijing, China. She is a post-doctoral of school of chemistry and chemical engineering at University of Jinan, Shandong, China. Her research interests focus on the construction of nanomaterials for fuel cell and biosensors with diseases, energy and environment applications.

Rong Ren joined Department of Mathematical Sciences from Zibo Normal College.

Yaoguang Wang received his BS degree in chemistry from University of Jinan in 2012, MS degree in chemical engineering and technology from University of Jinan in 2015 and PhD degree in chemical engineering and technology from University of Jinan in 2019. Now, he is an associate professor in Qilu University of Technology (Shandong Academy of Sciences). His main research interests are electrochemical sensors and biosensors.

Dawei Fan got her PhD from Lanzhou Institute of Chemical Physics, Chinese Academy of Sciences. Her main research interests are the construction of orderly self-assembled structures, research of photochemical and electrochemical sensors. He has published over 30 research papers including Angew. Chem. Int. Edit., Biosens. Bioelectron., J. Phys. Chem. C, Amino Acids, J. Colloid. Interf. Sci., Phys. Chem. Chem. Phys., Talanta.

Dan Wu a professor and received the DS degree from Shandong University in 2005. She dedicates to the surfactant and biological macromolecules interaction. And now she also studies the role of surfactant in electrochemical immunosensor.

Yu Du joined School of Chemistry and Chemical Engineering from University of Jinan.

Kun Xu is a current PhD student, studies in School of Chemistry and Chemical Engineering, University of Jinan. He is working on constructing immunosensor.

Xiang Ren received his BS degree in Chemistry of Materials from University of Jinan in 2012, M.S. degree in Chemical Engineering and Technology from University of Jinan in 2015 and PhD degree from University of Jinan/University of Electronic Science and Technology of China in 2019. Now, he is an associate professor in University of Jinan. His main research interests are energy catalysis, nanomaterials controlled-synthesis, and electrochemical biosensors.

Qin Wei a Professor and DSc has devoted herself to analytical teaching and scientific research. Her main research interests are the determination of protein and nucleic acid by photometry and the electrochemical immunosensor preparation. She has published over one hundred articles on analysis, immunosensor and applied successfully for many research projects, such as Biomaterials, Adv. Mater., Adv. Funct. Mater., Anal. Chem., Biosens. Bioelectron., Sens. Actuators B: Chem., Talanta.

Huangxian Ju received his BS, MS and Ph.D. degrees from Nanjing University during 1982–1992. He was a postdoc in Montreal University (Canada) from 1996 to 1997 and a guest professor in three universities of Germany and Ireland in 1999–2000. He became an associate and full professor of Nanjing University in 1993 and 1999. He is currently the director of State Key Laboratory of Analytical Chemistry for Life Science. His research interests focus on analytical biochemistry, biosensing and molecular diagnosis. He has published 616 papers in different journals with SCI h-index of 83 (29,523 citations) and Google Scholar h-index of 91 with more than 29000 citations.